Journal of ELECTRONIC MATERIALS, Vol. 44, No. 3, 2015
DOI: 10.1007/s11664-014-3593-4


# Use of Spherical Instrumented Indentation to Evaluate the Tensile Properties of 3D Combined Structures

WON-SEOK SONG,[1,3] SEUNG-GYU KIM,[1] YOUNG-CHEON KIM,[2] and DONGIL KWON[1]

1.—Department of Materials Science and Engineering, Seoul National University, Seoul 151-744, Republic of Korea. 2.—School of Materials Science and Engineering, UNIST (Ulsan National Institute of Science and Technology), Ulsan 689-798, Republic of Korea. 3.—e-mail: jenus04@snu.ac.kr

In this paper we propose a novel method, spherical indentation, for evaluation of the plastic properties of combined structures. Three-dimensional (3D) printed products, for example gradient metal alloys consisting of different kinds of material, contain interfaces that can act as weak points and threaten the mechanical reliability of products. Combined structures containing an interface between Cu alloy and Ag were prepared for testing. Samples were heat-treated at 100°C and 200°C for 3 h to optimize processing conditions. The indentation tensile properties of the samples were estimated by analyzing multiple loading–unloading curves obtained by use of the representative stress and strain method. A continuous increase in both yield strength and tensile strength was observed for the Cu alloy and the Cu/Ag interface after heat treatment at up to 200°C, because of precipitation hardening. These experimental results show that mechanical characterization of combined structures by spherical indentation is highly useful on the nano and micro scales.

**Key words:** Spherical indentation, tensile properties, representative stress and strain, combined structure

## INTRODUCTION

In manufacturing industry, 3D printing technology has the potential to become an economic breakthrough that makes process and material consumption more efficient than traditional manufacturing methods with such complex cycles as casting, rolling, and cutting. Because this technology can be utilized in a wide range of industries from health care to manufacture, the number of fields in which 3D printing is used is steadily increasing.[1–3] Metal-based 3D printing has recently attracted much attention. However, it is known that the mechanical properties of 3D-printing-based products are strongly affected by, for example, manufacturing process, loading direction, and post heat treatment.[4,5] In particular, the interface between different materials in products such as gradient metal alloys (GMA) can threaten mechanical reliability. It is, thus, necessary to verify the mechanical properties of the products on the micro and nano scales.[4,6] However, conventional tests, for example the tensile test and crack tip opening displacement are difficult to apply to nano and micro structures, because of size limitations. Recently, nano-indentation has become prominent as an alternative method of mechanical testing on the nano and micro scales. A variety of mechanical properties can be derived from the load–displacement curve, which continuously records indentation displacement and load at an indenter. Initially, this method could only be used to evaluate elastic modulus and hardness;[7,8] now, however, it has been broadened to handle residual stress,[9,10] viscoelasticity,[11,12] fracture toughness,[13] and indentation tensile properties.[14,15]

(Received July 15, 2014; accepted December 10, 2014; published online January 8, 2015)

In this study, spherical instrumented indentation was used to evaluate the tensile properties of combined structures. The samples were three kinds of 7-$\mu$m-thick layer: Cu alloy, Ag, and the Cu/Ag interface. Heat treatment of the samples was conducted to find the optimum process conditions, for example temperature and time. By use of the representative stress and strain approach, yield strength and tensile strength were extracted from multiple loading–unloading curves. The tensile properties of the samples were compared for different testing location and heat-treatment conditions.

## THEORETICAL BACKGROUND

Determining the precise contact displacement is an important step, because indentation tensile properties are very dependent on it. Real contact displacement $h_c$ can be calculated by considering not only peak displacement $h_{max}$ in the load–displacement curve but also the elastic deflection $h_d$[8] and plastic pile-up $h_p$ that occur around the indenter at the moment of indentation[14]:

$$h_c = h_{max} - h_d + h_p. \quad (1)$$

On the basis of the geometrical shape of the indenter, the contact radius $a_c$ and contact area $A_c$ of a material can be calculated from the contact displacement $h_c$ and indenter radius $R$.

It is well known that the relationship between representative stress, $\sigma_r$, and mean pressure, $P_m$, is[16]:

$$\sigma_r = \left(\frac{1}{\psi}\right)P_m = \left(\frac{1}{\psi}\right)\left(\frac{L_{max}}{A_c}\right), \quad (2)$$

where $\psi$ is a plastic constraint factor and $L_{max}$ is the peak load. Here a constant value of 3.0 was used for $\psi$ on the basis of slip line theory, as verified for a variety of materials by use of finite element analysis.[17]

The representative strain is defined by analyzing the strain in the lower part of the spherical indenter[14]:

$$\varepsilon_r = \left(\frac{\alpha}{\sqrt{1-(a_c/R)^2}}\right)\left(\frac{a_c}{R}\right). \quad (3)$$

The shear strain was derived by defining and differentiating the displacement in the direction of the indentation axis, and the proportional constant $\alpha$ was determined as 0.14 by finite-element analysis. A schematic diagram of the procedure for determining tensile properties, i.e. yield strength and tensile strength, is shown in Fig. 1.[18] Representative stress and strain were obtained by constructing several loading–unloading curves, then fitting these by use of constitutive equations. A Hollomon-type equation was used for common metallic materials for which power-law hardening is observed. Yield strength was determined as the intercept of the flow curve with the slope of elastic modulus, 0.2% offset from the origin. The ultimate tensile strength can be calculated by using the relationship with the strain-hardening exponent and ultimate tensile strain from the theory of instability in tension.[19]

## EXPERIMENTAL

Combined-structure Cu alloy/Ag samples 7 $\mu$m thick were prepared for nanoindentation. The chemical composition of the Cu alloy is summarized in Table I. For electronic devices, extension of the operating temperature range to 200°C is necessary, as is enhancement of package reliability. Samples were heat treated at 100°C and 200°C for 3 h, followed by furnace cooling. After heat treatment, all specimen surfaces were mechanically ground with emery paper and finely polished with 0.1 $\mu$m alumina powder. Nanoindentation tests were conducted by use of the Nanoindenter XP (MTS Systems, Oak Ridge, TN, USA) with load resolution 50 nN and displacement resolution 0.01 nm. The maximum depth was 180 nm with sixfold unloading to zero load. A diamond sphero-conical indenter with tip radius 1 $\mu$m was used. The distance between two indents was 5 $\mu$m, to avoid interaction between indentation tests. To minimize extrinsic effects, thermal drift was controlled below 0.02 nm/s and indenter blunting was taken into account by area calibration, by use of fused quartz. A schematic

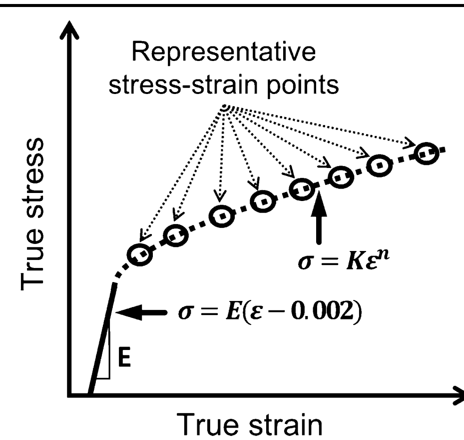


Fig. 1. Schematic diagram of the procedure for determining tensile properties by use of the representative stress and strain approach.[18]

**Table I. Composition of the Cu alloy in the Cu/Ag combined structure**

| Element | Cu | Si | Ni | Mg | Total |
|---|---|---|---|---|---|
| wt.% | 96.2 | 0.65 | 3 | 0.15 | 100 |

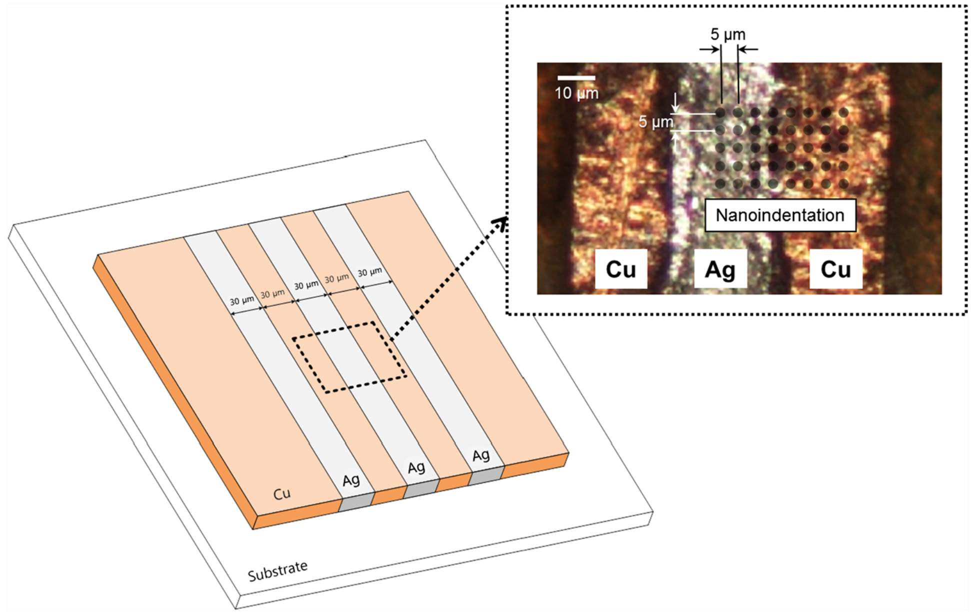


Fig. 2. Schematic diagram of Cu/Ag combined structure and test positions.

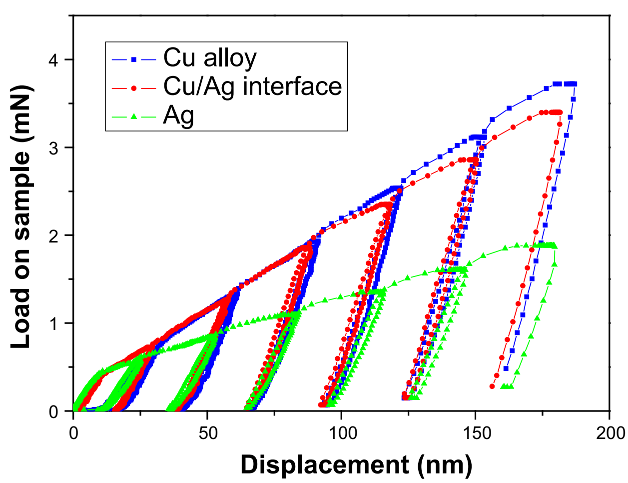


Fig. 3. Multiple loading and unloading curves from spherical indentation at room temperature.

diagram of specimen and the test positions is shown in Fig. 2.

## RESULTS AND DISCUSSION

Figure 3 shows multiple plots of loading–unloading as a function of displacement at room temperature for combined-structure Cu/Ag samples. As is apparent from Fig. 3, the sample can be broken down into three parts, Cu alloy, Ag, and Cu/Ag interface, because distinct load differences are observed for each part at fixed displacement. Loading and unloading curves for combined-structure samples with three heat-treatment conditions, 100°C or 200°C for 3 h or no heat treatment, were analyzed to evaluate tensile properties by use of a

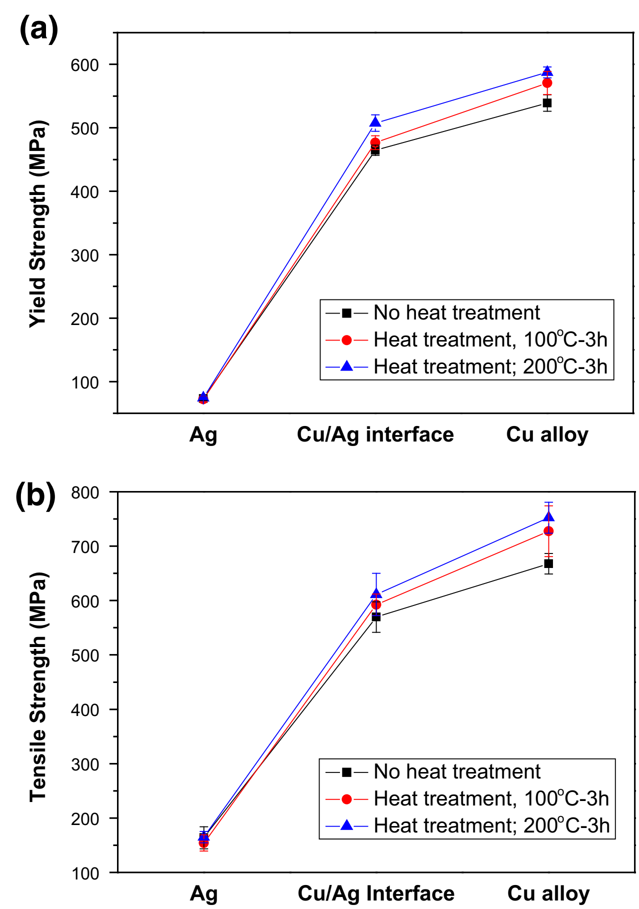


Fig. 4. Yield strength (a) and tensile strength (b) of Cu alloy, Cu/Ag interface, and Ag as a function of heat-treatment conditions, determined by use of spherical indentation.

**Table II. Mechanical properties (by spherical indentation) of Cu Alloy/Ag combined structure after no-heat treatment and after heat treatment for 3 h**

| | Yield strength (MPa) | | | Tensile strength (MPa) | | |
|---|---|---|---|---|---|---|
| Heat-treatment temperature (°C) | Ag | Interface | Cu alloy | Ag | Interface | Cu alloy |
| No heat treatment | 73 ± 3 | 465 ± 8 | 539 ± 13 | 164 ± 20 | 570 ± 28 | 668 ± 19 |
| 100 | 72 ± 4 | 476 ± 11 | 571 ± 18 | 154 ± 15 | 592 ± 20 | 727 ± 47 |
| 200 | 74 ± 2 | 506 ± 13 | 587 ± 9 | 165 ± 10 | 611 ± 39 | 752 ± 28 |

representative stress and strain method. Figure 4 compares yield strength and tensile strength for each position and heat-treatment conditions; Table II shows the resulting mechanical properties. Theoretical analysis and finite element methods for the elastic–plastic indentation stress field associated with an indenter were performed to establish the relationship between indentation hardness and uniaxial strength.[20,21] Moreover, work focused on the accuracy of tensile properties resulting from spherical indentation and tried to compare these with the properties of bulk metal.[18,22] In this experiment, the yield strengths of the Cu alloy and Ag by indentation at room temperature were, respectively, 539 ± 13 MPa and 73 ± 3 MPa; the room-temperature tensile strengths of the Cu alloy and Ag were 668 ± 19 MPa and 164 ± 20 MPa. Comparison of these indentation values with those in the literature derived by tensile testing[23,24] yields a ±15% error range between the two, showing that the tensile properties from this experiment correlate well with those from standard tensile testing.

The results in Fig. 4 can be used to represent mechanical behavior on the nano and/or micro scale. For the Cu alloy, both yield and tensile strength increase continuously with increasing heat-treatment temperature until 200°C. The yield and tensile strength of the Cu alloy heat treated at 200°C are approximately 10% greater than that of the Cu alloy with no heat treatment. This difference is because of precipitation hardening, which occurs frequently for copper–nickel–silicon. From these experimental results it is apparent that the properties of the Cu alloy layer in the sample can be enhanced by heat treatment between room temperature and at least 200°C.

It is important to assess the mechanical properties of the interface because that is where fracture is usually initiated. However, it is extremely difficult to test because of its small width. One of the advantages of indentation is that it enables such small-scale testing, and the results of this experiment proved it is true here also. The mechanical properties the Cu alloy–Ag interface increased similarly to those of the Cu alloy as a function of heat-treatment temperature. The interface has somewhat poorer mechanical properties than the Cu, in accordance with the rule of mixtures between Cu alloy and Ag. It is expected that recovery and recrystallization will be induced, leading to a decrease in yield/tensile strength after heat treatment at temperatures >500–700°C. The yield-strength and tensile-strength of Ag were not significantly different after heat treatment: because the Ag layer in the combined structure is of high purity, its thermal stability is greater than that of the other components.

## CONCLUSIONS

In this study, nanoindentation experiments using a spherical indenter were performed on Cu/Ag combined structures to evaluate their mechanical behavior. The yield strength and tensile strength, regarded as the most fundamental mechanical properties, were evaluated from multiple loading–unloading curves by using the representative stress and strain approach. Hardening behavior was observed for the Cu alloy and the Cu/Ag interface after heat treatment at 100°C and 200°C, because of precipitation hardening, whereas the mechanical properties of pure silver were not affected. Spherical indentation was successfully used for local evaluation of the mechanical reliability of complex structures, and can be used to determine optimum processing conditions, for example heat-treatment temperature and time, on the micro and nano scales.

## ACKNOWLEDGEMENTS

This work was supported by the National Research Foundation of Korea (NRF) Grant funded by the Korea government (MSIP) (2010-0029211).

## REFERENCES

1. METI Journal, The potential of 3D printing. (METI Journal, 2013) http://www.meti.go.jp/english/publications/pdf/journal2013_08a.pdf. August 2013.
2. I.D. Harris, Development and Implementation of Metals Additive Manufacturing (Deep Offshore Technology, 2011), http://ewi.org/eto/wp-content/uploads/2013/06/Additive-Manufacturing-DOT-Paper-2011.pdf. 2011.
3. I. Gibson, D.W. Rosen, and B. Stucker, Additive Manufacturing Technologies (Springer, Dordrecht, 2010), pp. 6–11, pp. 32–38.
4. I. Shishkovsky, F. Missemer, N. Kakovkina, and I. Smurov, *Crystals* 3, 517 (2013).
5. S. Copley, R. Martukanitz, W. Frazier, and M. Rigdon, Mechanical Properties of Parts Formed by Laser Additive Manufacturing (Advanced Materials & Processes, 2011), http://www.asminternational.org/documents/10192/1904083/

amp16909p26.pdf/c31656cc-06c3-4642-bca6-d45c20c49b07. September 2011.
6. D.C. Hofmann, S. Roberts, R. Otis, J. Kolodziejska, R.P. Dillon, J.-O. Suh, A.A. Shapiro, Z.-K. Liu, and J.-P. Borgonia, *Sci. Rep.* (2014). doi:10.1038/srep053571.
7. M.F. Doerner and W.D. Nix, *J. Mater. Res.* 1, 601 (1986).
8. W.C. Oliver and G.M. Pharr, *J. Mater. Res.* 7, 1564 (1992).
9. S. Suresh and A.E. Giannakopoulos, *Acta Mater.* 46, 5755 (1998).
10. Y.H. Lee and D. Kwon, *J. Mater. Res.* 17, 901 (2002).
11. S.A.S. Asif, K.J. Wahl, and R.J. Colton, *Rev. Sci. Inst.* 70, 2408 (1999).
12. D.M. Shinozaki and Y. Lu, *J. Elect. Mater.* 26, 852 (1997).
13. J. Malzbender and G. de With, *Surf. Technol.* 135, 60 (2000).
14. X.Z. Hu and B.R. Lawn, *Thin Solid Films* 322, 225 (1998).
15. J.-H. Ahn and D. Kwon, *J. Mater. Res.* 16, 3170 (2001).
16. D. Tabor, *Hardness of Metals* (Oxford: Clarendon Press, 1951), p. 37.
17. E.-C. Jeon, M.-K. Baik, S.-H. Kim, B.-W. Lee, and D. Kwon, *Key Eng. Mater.* 297–300, 2152 (2005).
18. J.-Y. Kim, et al., *Surf. Coat. Technol.* 201, 4278 (2006).
19. G.E. Dieter, *Mechanical Metallurgy* (New York: McGraw Hill, 1986), p. 289.
20. C. Hardy, et al., *J. Numer. Met. Eng.* 3, 451 (1971).
21. K.L. Johnson, *J. Mech. Phys. Solids* 18, 115 (1970).
22. K.-W. Lee, et al., *J. Phys. D* 41, 074014 (2008).
23. A.M. Howatson, P.G. Lund, and J.D. Todd, *Engineering Tables and Data* (Netherlands: Springer, 1972), p. 41.
24. Y.V. Murty, *Encycl. Mater.* 2, 2483 (2008).